1-1-2019

pIRIR and IR-RF dating of archaeological deposits at Badahlin and Gu Myaung Caves - First luminescence ages for Myanmar

Maria Schaarschmidt
University of Wollongong, ms648@uowmail.edu.au

Xiao Fu
University of Wollongong, xiaofu@uow.edu.au

Bo Li
University of Wollongong, bli@uow.edu.au

Ben Marwick
University of Washington, bmarwick@uow.edu.au

Kyaw Khaing
Department of Archaeology and National Museum, Ministry of Religious Affairs and Culture

See next page for additional authors

pIRIR and IR-RF dating of archaeological deposits at Badahlin and Gu Myaung Caves - First luminescence ages for Myanmar

Abstract

Reliable chronologies are essential for understanding the timing and routes of human dispersal through Southeast Asia, both of which remain open questions. This study provides luminescence chronologies for two archaeological sites in Myanmar-Badahlin Cave and Gu Myaung Cave-from which Palaeolithic artefacts have been recovered. We applied single-grain post-infrared infrared stimulated luminescence (pIRIR) and multi-grain infrared-radiofluorescence (IR-RF) dating methods to potassium-rich feldspar (K-feldspar) grains extracted from the sedimentary deposits at these two sites. Luminescence characteristics of the K-feldspar extracts showed that the procedures were well suited for dating. The single-grain pIRIR ages suggest human occupation of Badahlin and Gu Myaung Caves by ~30 ka and ~25 ka, respectively, although the age estimates for Gu Myaung Cave are much older than the radiocarbon ages. The ages obtained using the IR-RF signal are even older, which we attribute to insufficient bleaching of this signal-and perhaps also the pIRIR signal-and the probable existence of a substantial residual dose at the time of sediment deposition.

Keywords

luminescence, first, -, caves, myaung, gu, badahlin, ages, deposits, myanmar, archaeological, dating, ir-rf, pirir

Publication Details

Schaarschmidt, M., Fu, X., Li, B., Marwick, B., Khaing, K., Douka, K. & Roberts, R. G. (2019). pIRIR and IR-RF dating of archaeological deposits at Badahlin and Gu Myaung Caves - First luminescence ages for Myanmar. Quaternary Geochronology, 49 262-270.

Authors

Maria Schaarschmidt, Xiao Fu, Bo Li, Ben Marwick, Kyaw Khaing, Katerina Douka, and Richard G. Roberts

pIRIR and IR-RF dating of archaeological deposits at Badahlin and Gu Myaung Caves – first luminescence ages for Myanmar

Maria Schaarschmidt[a*], Xiao Fu[a], Bo Li[a,b], Ben Marwick[a,c], Kyaw Khaing[d], Katerina Douka[e], Richard G. Roberts[a,b]

[a] Centre for Archaeological Science, School of Earth and Environmental Sciences, University of Wollongong, Wollongong, NSW 2522, Australia

[b] ARC Centre of Excellence for Australian Biodiversity and Heritage, University of Wollongong, Wollongong, NSW 2522, Australia

[c] Department of Anthropology, University of Washington, Seattle, WA 98195, USA

[d] Field School of Archaeology, Pyay, Department of Archaeology and National Museum, Ministry of Religious Affairs and Culture, Myanmar

[e] Research Laboratory for Archaeology and the History of Art, University of Oxford, Oxford OX1 3QY, UK

* Corresponding author: ms648@uowmail.edu.au

Abstract

Reliable chronologies are essential for understanding the timing and routes of human dispersal through Southeast Asia, both of which remain open questions. This study provides luminescence chronologies for two archaeological sites in Myanmar—Badahlin Cave and Gu Myaung Cave—from which Palaeolithic artefacts have been recovered. We applied single-grain post-infrared infrared stimulated luminescence (pIRIR) and multi-grain infrared-radiofluorescence (IR-RF) dating methods to potassium-rich feldspar (K-feldspar) grains extracted from the sedimentary deposits at these two sites. Luminescence characteristics of the K-feldspar extracts showed that the procedures were well suited for dating. The single-grain pIRIR ages suggest human occupation of Badahlin and Gu Myaung Caves by ~30 ka and ~25 ka, respectively, although the age estimates for Gu Myaung Cave are much older than the radiocarbon ages. The ages obtained using the IR-RF signal are even older, which we attribute to insufficient bleaching of this signal—and perhaps also the pIRIR signal—and the probable existence of a substantial residual dose at the time of sediment deposition.

***Keywords**: K-feldspar, single grains, post-IR IRSL, radiofluorescence, partial bleaching, residual dose, Southeast Asia*

1 Introduction

Badahlin and Gu Myaung Caves both lie at the foot of the Shan Plateau, which stretches eastward from central Myanmar into northern Thailand (Fig. 1). Badahlin Cave was first excavated in 1969 (Aung Thaw, 1971), when stone artefacts and animal bones were recovered. Radiocarbon (^{14}C) dating indicated a maximum age for the cultural materials of ~13,400 years BP (Aung-Thwin, 2001). In 2013, we conducted a 2.5 m-deep excavation at Badahlin Cave 2, which is separate from the site of Badahlin Cave 1 where the earlier excavations were undertaken. We also conducted a 4 m-deep excavation at Gu Myaung Cave, which had not previously been excavated, and collected three charcoal samples that gave ^{14}C ages ranging from ~3 to ~15 ka cal BP (Table S3). The ^{14}C ages for Badahlin Cave 1 and Gu Myaung Cave provide preliminary—and likely minimum—age constraints for these two sites, which have yielded Palaeolithic artefacts. Additional data are needed to test these chronologies and extend them into the deeper deposits.

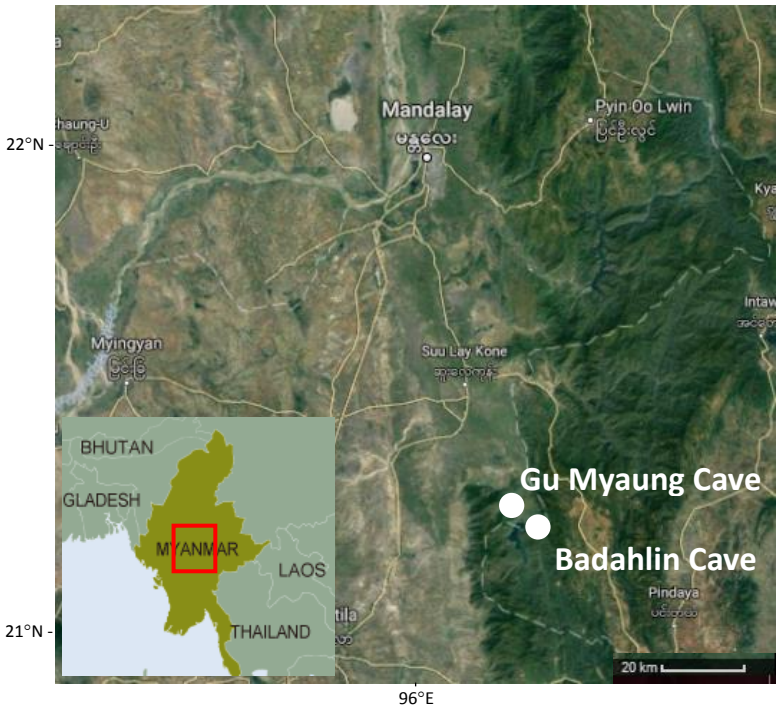

Figure 1. Map of central Myanmar showing the locations of the two study sites.

Luminescence dating has been used previously to date archaeological sites in mainland Southeast Asia. Although conventional optically stimulated luminescence (OSL) dating of quartz has been applied to some sites (e.g., Demeter et al., 2015; Forestier et al., 2015; Moncel et al., 2016), the utility of quartz OSL is commonly limited due to signal saturation or low intrinsic grain brightness (Roberts et al., 2005; Jacobs and Roberts, 2007). We encountered these difficulties using the quartz OSL signal during our initial tests of the sediment samples collected from Badahlin and Gu Myaung Caves. Consequently, alternative minerals, luminescence signals and dating procedures were required. In this study, we have used two luminescence signals—single-grain post-infrared infrared stimulated luminescence (pIRIR) and multi-grain infrared radiofluorescence (IR-RF)—to estimate the depositional age of sand-sized grains of potassium-rich feldspar (K-feldspar). Here we report the preliminary results of our investigations to augment the ^{14}C chronologies for these two human occupation sites. To our knowledge, these are the first luminescence ages for archaeological sites in Myanmar (Aung et al., 2015).

2 Site and sample descriptions

2.1 Study sites

Badahlin Cave (21.13274°N, 96.34032°E) and Gu Myaung Cave (21.20156°N, 96.31926°E) are located in central Myanmar (Fig. 1). They are formed in Permian and Permo-Triassic limestone, which contains a number of karstic features, including sinkholes and phreatic tubes.

Badahlin Cave was formed phreatically and consists of several inter-connecting chambers. The cave roof is ~30 m thick and speleothems are abundant, with occasional roof collapses facilitating entry routes for humans into the cave complex. In one of the chambers, we excavated a location close to the wall to a depth of ~2.5 m (Fig. 2a); excavation details will be presented in a forthcoming archaeological report. The deposit is composed mainly of dark sandy silt that becomes enriched in clay with increasing depth. The sediment layers dip at a low angle towards the cave wall and the deposit is moist throughout, with a slight increase in moisture with depth.

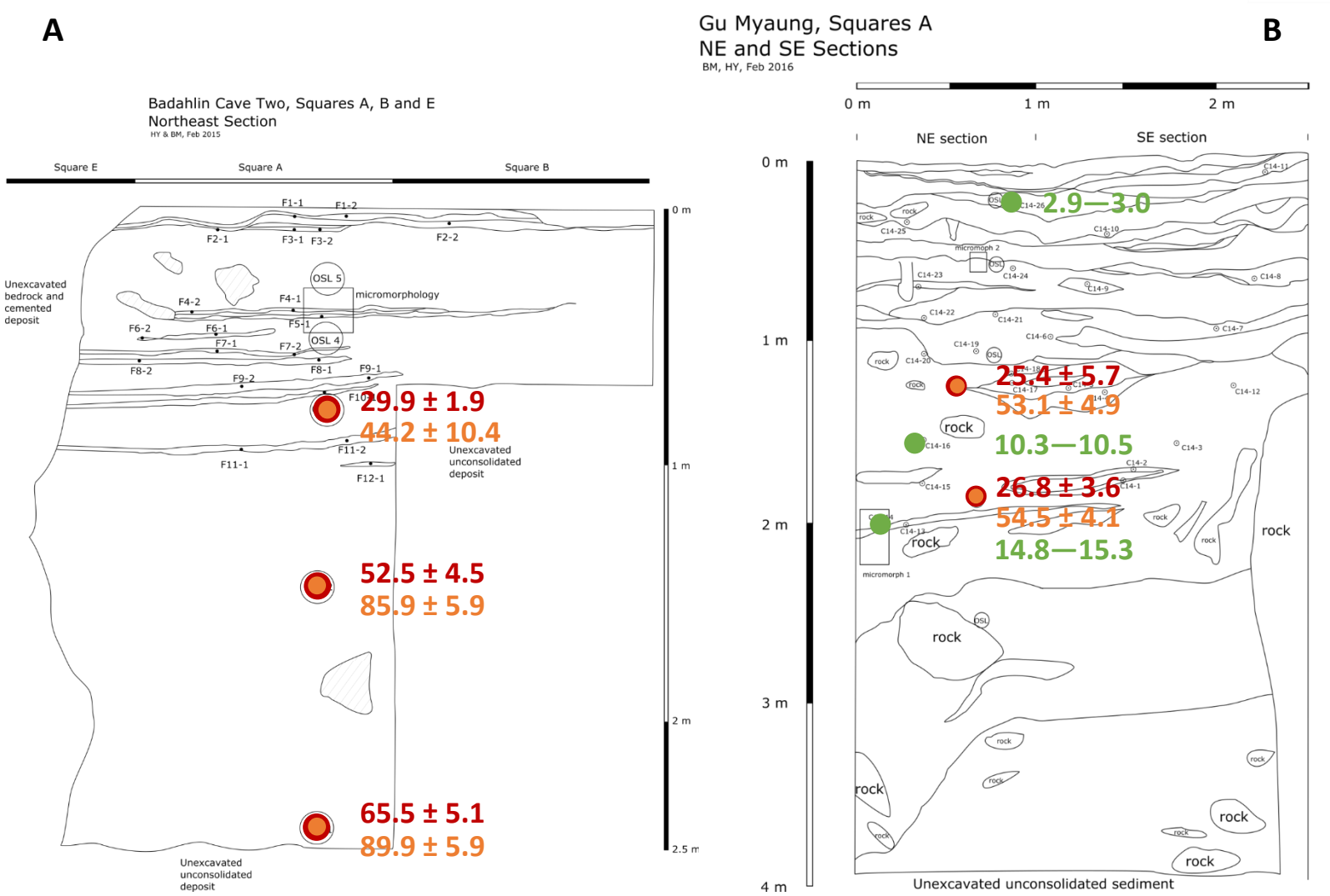

Figure 2. Section drawings of excavated sections at Badahlin Cave (A) and Gu Myaung Cave (B), showing pIRIR ages (red), IR-RF ages (IRSAR, orange) and calibrated ^{14}C age ranges (green). The pIRIR and IR-RF ages (± 1σ uncertainties) are in ka, and the ^{14}C age ranges (95.4% confidence interval) are in ka cal BP.

In the upper part of the sequence (i.e., the top ~1 m), sediment layers are interspersed by thin flowstones. Calcified sediment and limestone inclusions were also found occasionally, the latter being usually cobble to pebble sized and irregularly shaped. Two excavations were undertaken: squares A, B and E relate to the first of these, and squares C and D to the second.

Gu Myaung Cave is also a phreatically formed limestone cave, which overlooks the Panlaung River. We excavated just inside the cave mouth to a depth of ~4 m (Fig. 2b); excavation details will be provided in an archaeological report in preparation. The upper ~1.5 m of deposit consists mostly of horizontally layered grey-brown silt with some clay and gravel, and hearth features with abundant white ash and charcoal. Boundaries between layers are well-defined, probably due to the short time since deposition and the lack of post-depositional disturbance. The number of hearth features declines below this depth, resulting in a less heterogeneous and structured deposit. Below a depth of ~2 m, no stratigraphic features are readily apparent and the deposit is enriched with clay and contains occasional large rocks.

2.2 Sediment samples

Samples were collected using light-safe steel tubes, 22 cm in length and 5 cm in diameter. *In situ* measurements of the gamma-ray dose rate were made at each sample location by inserting a NaI(Tl) detector into the empty tube holes, and additional bags of sediment were collected from these holes for beta dose rate and moisture content measurements in the laboratory. Samples from Badahlin Cave were collected from relatively moist sediments in square A of the northeast section of the excavation, from 80, 150 and 240 cm depth below surface (Fig. 2a). Samples from Gu Myaung Cave were collected from the sediments in the northeast section of the excavation, from 140 cm and 202 cm depth below surface (Fig. 2b). The uppermost sample at each site coincides with the depth of the lowest artefact found during excavation. The other samples were collected from the underlying archaeologically sterile layers and were analysed to investigate the longer-term history of sediment deposition in these caves.

3 Methods

3.1 Sample preparation and instrumentation

Samples were prepared using standard methods—including wet-sieving, HCl acid and H_2O_2 treatments, and density separations—to isolate sand-sized grains (90–125 µm and 180–212 µm in diameter) of quartz and K-feldspar. Our initial investigations of individual quartz grains (180–212 µm in diameter) revealed that their inherent OSL signals (i.e., their response to a test dose) were very weak or their natural OSL signals were in saturation. Accordingly, we concentrated thereafter on K-feldspar grains of the same or smaller (90–125 µm) grain size, isolating them using a sodium polytungstate solution with a density of 2.58 g/cm^3 and then etching them in 10% HF acid for 10 min to remove the alpha-dosed outer layer.

All pIRIR measurements were carried out on Risø TL-DA-20 readers equipped with bialkali photomultiplier tubes (Electron Tubes Ltd 9235QB), blue-transmission filter packs (Schott BG 39 and Corning 7-59), infrared (IR) light-emitting diodes and lasers, and calibrated ^{90}Sr/^{90}Y beta sources (Bøtter-Jensen et al., 2003). Grains were loaded on to discs drilled with 100 holes, each 300 µm in depth and 300 µm in diameter, and each hole position was calibrated for its beta dose rate. For relevant experiments, samples were bleached using an external solar simulator (Dr Hönle UVACUBE 400). The IR-RF measurements were made on aliquots of ~2 mm in diameter (corresponding to a monolayer of between ~70 and ~230 grains, depending on the grain size) using a Freiberg Instruments Lexsyg research reader equipped with a photomultiplier tube sensitive in the near-IR (Hamamatsu H7421-50), a Chroma-D850/40 interference filter, a light source with different wavelengths and a ^{90}Sr/^{90}Y beta source (Richter et al., 2012, 2013). The Lexsyg also has an in-built solar simulator, which we used for all bleaching steps during IR-RF measurements.

3.2 Environmental dose rates

Beta dose rates for dried and powdered sub-samples of the sediments collected in the field were measured using a Risø GM-25-5 beta counter (Bøtter-Jensen and Mejdahl, 1988) and the procedures described in Jacobs and Roberts (2015). The gamma dose rates were measured in the field using an Exploranium GR-320 EnviSpec gamma spectrometer, and the cosmic-ray dose rates were estimated following Prescott and Hutton (1994). Adjustments were made for beta-dose attenuation (Guérin et al., 2012) and for the effect of moisture content on the external beta, gamma and cosmic-ray dose rates (Readhead, 1987; Nathan and Mauz, 2008). The measured (field) water contents were used for each sample and assigned a relative uncertainty of ± 25% (at 1σ) to accommodate any likely variations over the period of sample burial. The internal dose rate can be a significant contributor to the total dose rate for K-feldspar: we assumed an internal potassium content of 10 ±

2% (Smedley et al., 2012) and an internal Rb content of 400 ± 100 μg/g (Huntley and Hancock, 2001), resulting in estimated internal dose rates of 0.38 ± 0.08 and 0.67 ± 0.12 Gy/ka for grains of 90–125 and 180–212 μm diameter, respectively.

3.3 pIRIR measurement procedures

The pIRIR signal measured at elevated temperature has been reported to suffer much less from anomalous fading than the conventional IR stimulated luminescence (IRSL) signal measured at 50°C, and to possibly not fade at all (e.g., Li and Li, 2011; Buylaert et al., 2012b; Li et al., 2014; Roberts et al., 2015). However, it is also harder to bleach in natural sunlight than either the IRSL signal or the quartz OSL signal (e.g., Li and Li, 2011; Colarossi et al., 2015). Single-grain measurements, therefore, provide a useful means of examining the extent of bleaching of individual grains in any particular sample (e.g., Reimann et al., 2012; Trauerstein et al., 2014; Blegen et al., 2015; Rhodes, 2015) and to check if significant post-depositional mixing has occurred.

In this study, individual grains of K-feldspar were dated using a two-step single-grain pIRIR procedure (Blegen et al., 2015). In this procedure (Table S1), the initial IR stimulation is performed at 200°C for 100 s using light-emitting diodes to stimulate all grains simultaneously; the pIRIR dating signals from individual grains are then measured at 275°C using a focused IR laser beam for stimulation. A preheat of 320°C for 60 s was applied to the natural, regenerative and test doses; we used a test dose ~40% of the size of the expected natural dose. These parameters were chosen on the basis of dose recovery tests (Galbraith et al., 1999), as described below. To eliminate grains with luminescence properties unsuitable for the pIRIR procedure, we applied standard single-grain rejection criteria, following Blegen et al. (2015). Grains were rejected if: 1) the test dose signal measured during the natural dose cycle (T_n) was within 3σ of the background count; 2) the relative error on T_n exceeded 20%; 3) the 'recycling ratio' (i.e., the ratio between the sensitivity-corrected signals for a duplicate regenerative dose) was inconsistent with unity at 2σ; 4) the extent of 'recuperation' (i.e., the ratio between the sensitivity-corrected zero dose and natural dose signals) was greater than 5%; 5) the natural signal was equal to or higher than the saturation level of the dose response curve (DRC); and 6) the DRC could not be reliably fitted using a saturating exponential or an exponential-plus-linear function. For all accepted grains (i.e., those remaining after applying these rejection criteria), the equivalent dose (D_e) was estimated by projecting the sensitivity-corrected natural signal of each grain on to its corresponding sensitivity-corrected DRC.

3.4 IR-RF measurement procedures

Radioluminescence (RL) or radiofluorescence (RF) was first proposed as a dating technique in the late 1990s (Trautmann et al., 1998, 1999a) and recently revisited by Frouin et al. (2017). The method is based on the fluorescence signal emitted during irradiation (Trautmann et al., 1999b), which has been suggested to not fade (Krbetschek et al., 2000; Novothny et al., 2010). If so, then the IR-RF signal would provide a validation test of the pIRIR results. In this study, we applied the original single-aliquot IR-RF procedure of Erfurt and Krbetschek (2003) and the updated procedure of Frouin et al. (2017) to multi-grain aliquots of K-feldspar from our samples.

Erfurt and Krbetschek's procedure—hereafter referred to as IRSAR—has four steps: 1) measure the natural IR-RF signal; 2) perform a prolonged solar bleach to reset the IR-RF signal; 3) wait for the superposed phosphorescence signal to decay; and 4) irradiate and measure the regenerated IR-RF signal (Table S1). All measurements made using the IRSAR procedure were carried out at room temperature. The modified IR-RF procedure of Frouin et al. (2017)—hereafter referred to as RF_{70}—has a similar structure as the IRSAR procedure, but samples are measured and irradiated at an elevated temperature (70°C). To reach this temperature on the Lexsyg system, discs are required to be held at 70°C for 2 min before making IR-RF measurements. For both procedures, we adopted the solar bleach settings of Frouin et al. (2015), which are listed in the footnote to Table S1.

The D_e value for each aliquot was obtained by sliding the regenerated IR-RF signal on to the natural IR-RF signal horizontally and vertically to minimise the residuals using the **R** function *analyse_IRSAR.RF()* in the **R** 'Luminescence' package (Kreutzer et al., 2017).

4 Results

4.1 Environmental dose rates

The total dose rates for all samples are summarised in Table 1, with the details given in Table S2. The total dose rates for samples from Badahlin Cave range from ~2.4 to ~3.9 Gy/ka, with much lower dose rates for the samples from Gu Myaung Cave (~1.3 Gy/ka). The dose rates are dominated by the beta dose rate (0.6–2.1 Gy/ka), with gamma dose rates of 0.3–1.3 Gy/ka, internal dose rates of 0.4–0.7 Gy/ka (depending on grain size) and cosmic-ray dose rates of 0.02 Gy/ka or less (the latter at Badahlin Cave because of rock shielding). The

179 total dose rates for Badahlin Cave are two- or three-fold higher than for Gu Myaung Cave, which we attribute
180 primarily to the greater amount of low-radioactivity carbonate in the latter samples. This is reflected in the U
181 and Th concentrations measured by field gamma spectrometry, which differ significantly between the two
182 sites: ~5 μg/g U and ~7 μg/g Th at Badahlin Cave, compared to ~0.4 μg/g U and ~3.3 μg/g Th at Gu Myaung
183 Cave.

184 **4.2 Single-grain pIRIR**

185 A representative single-grain pIRIR decay curve and the corresponding DRC for an accepted K-feldspar grain
186 from sample BDL2-OSL 2 are shown in Fig. S1. We conducted single-grain dose recovery tests on 3–5 discs of
187 one sample from each site (BDL2-OSL 2 and GUMY-OSL 3) to validate the pIRIR experimental conditions used
188 here for dating. Grains were bleached for 4 hr under the solar simulator to empty them of their natural doses,
189 and then given a beta dose (as a surrogate natural dose) of 236 Gy or 30 Gy, respectively, before being
190 measured using the pIRIR procedure in Table S1. The respective weighted-mean dose recovery ratios (i.e., the
191 ratio of measured dose to given dose) are 1.06 ± 0.04 and 0.97 ± 0.07, with dose overdispersion (OD) values of
192 27 ± 3% and 31 ± 6% (Fig. S2). To examine the anomalous fading rate of the pIRIR signal, we estimated *g*-values
193 for each sample using single (multi-grain) aliquots, following Auclair et al. (2003). The results obtained for
194 storage periods of up to 2 weeks (Fig. S3) indicate that the *g*-values vary from ~0 to 0.3 % per decade which
195 suggests that the pIRIR signals in these samples do not fade significantly—at least not on laboratory
196 timescales. This finding is consistent with previous studies that used an initial IR stimulation at 200°C to
197 effectively remove the fading component (e.g., Li and Li, 2012; Fu, 2014; Blegen et al., 2015; Yi et al., 2016).

198 The pIRIR signal has been shown to be relatively hard to bleach, with a residual dose of several Gy remaining
199 even after prolonged bleaching in sunlight (e.g., Li and Li, 2011; Buylaert et al., 2012b). To estimate the size of
200 any residual dose at the time of sediment deposition, and correct for it, we measured the dose values for 100–
201 300 natural grains of each sample after bleaching them for 4 hr in the solar simulator. The weighted-mean
202 residual dose for the Badahlin Cave samples is 7 ± 2 Gy, and 0.01 ± 6 Gy for samples from Gu Myaung Cave.
203 These residual doses are small to negligible compared with the measured D_e values of these samples, but we
204 nonetheless subtracted them to obtain the final D_e values for age determination. In summary, the factors
205 discussed above indicate that the pIRIR procedure is well-suited to our samples.

206 D_e values were determined using 180–212 μm grains for two of the Badahlin Cave samples and 90–125 μm
207 grains for both samples from Gu Myaung Cave, owing to the scarcity of larger grains; both grain-size fractions
208 were measured for sample BDL2-OSL 3, as a methodological cross-check. The number of grains—or pseudo-
209 single-grain measurements for the Gu Myaung Cave samples (~5 grains per hole)—that passed the rejection
210 criteria corresponds to between 2% and 27% of the total number of grains measured (Table 1). Most of the
211 grains were rejected based on the first criterion (low intrinsic brightness).

212

213

214

215

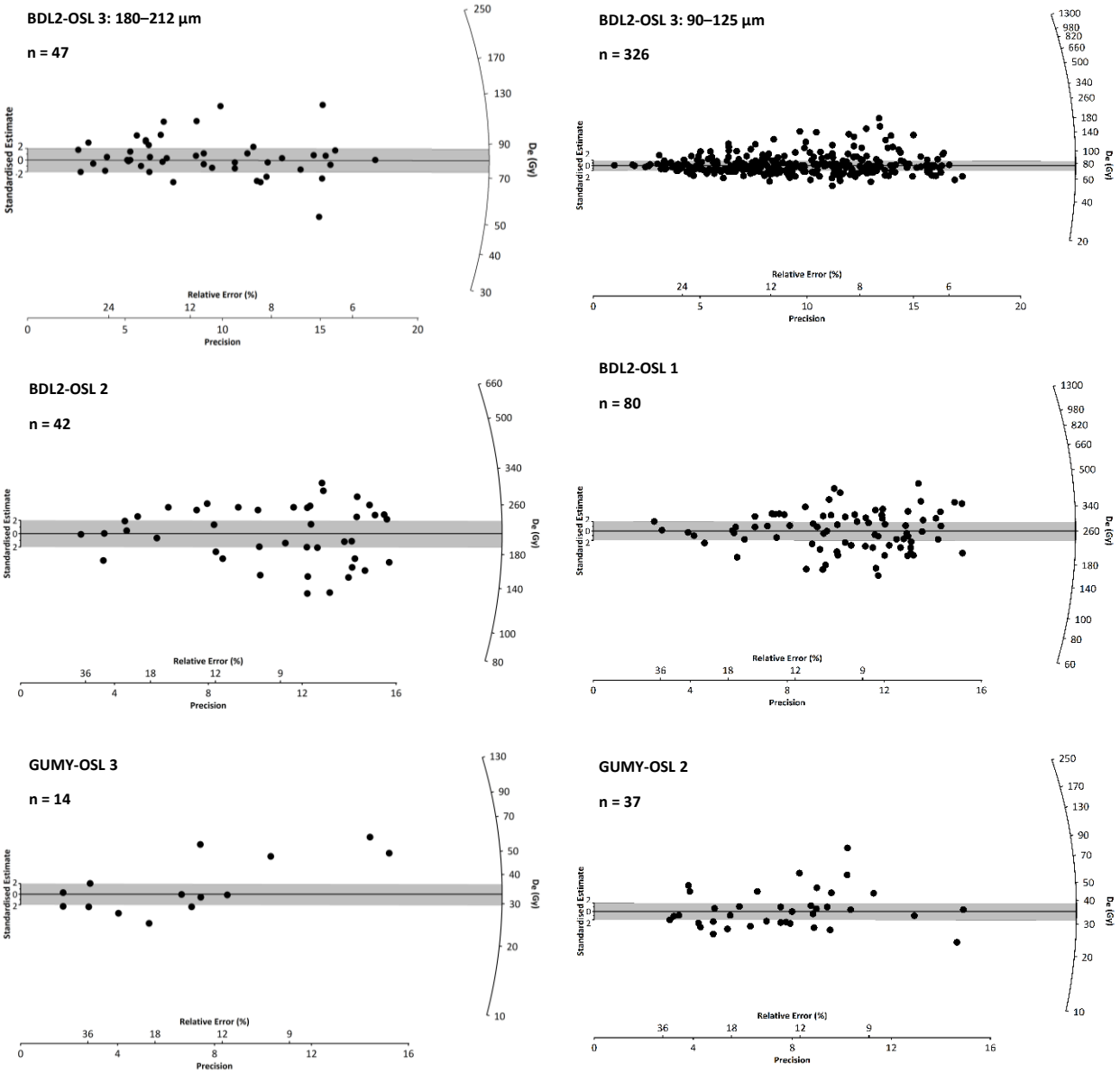

216 *Figure 3. Single-grain pIRIR D_e distributions for all samples. The grey bands are centred on the*
217 *weighted-mean D_e values estimated using the central age model; n = number of individual D_e values.*

218

The D_e distributions (Fig. 3) show some overdispersion in individual values, with OD values of 35 ± 4% to 39 ± 3% for the Badahlin Cave samples and 61 ± 8% and 70 ± 15% for GUMY-OSL 2 and GUMY-OSL 3, respectively. Most of the D_e overdispersion in the Badahlin Cave samples, and a large fraction of that observed in the Gu Myaung Cave samples, can be explained by intrinsic factors, as suggested by the high OD values (~27% and ~31%) obtained in the dose recovery tests (Fig. S2). The additional spread in the Gu Myaung Cave distributions could reflect incomplete bleaching during the last sediment transport event, beta microdosimetry variations, post-depositional mixing (although the stratigraphic sequence suggests a lack of disturbance) and/or the effects of non-identical bleaching and irradiation conditions in the laboratory and field (Galbraith et al., 2005). Both Gu Myaung Cave samples have small D_e datasets, however, so the OD values will be more sensitive to outliers in the D_e distributions.

The D_e distributions are broadly symmetrical, with values spread more or less equally above and below the central estimate. There are no indications of post-depositional mixing or partial bleaching—that is, no discrete populations of D_e values are evident, nor do the D_e values cluster at low doses with a 'tail' extending to high doses. The sole exception is the 90–125 μm D_e distribution of BDL2-OSL 3, which has a tail of D_e values extending to >300 Gy that could be interpreted as evidence of partial bleaching. This dataset is by far the largest of any of our samples, so such grains (which represent fewer than 10% of the total number) could also be present in the other samples, but are less conspicuous due to their low abundance. However, while the 180–212 μm D_e distribution of BDL2-OSL 3 contains a few grains with D_e values >100 Gy, it does not exhibit the same pattern of spread as observed for the 90–125 μm fraction and the weighted-mean ages for these two grain-size fractions are statistically indistinguishable (Table 1). This suggests that, even if some of the grains had been partially bleached, the net effect is not significant.

Based on these observations and interpretations, we calculated the D_e values for our samples using the central age model (CAM), which gives an estimate of the weighted geometric mean (Galbraith et al., 1999; Galbraith and Roberts, 2012). The final ages for the three samples from Badahlin Cave are in stratigraphic order and range from 30 ± 2 ka to 66 ± 5 ka, while both samples from Gu Myaung Cave are ~26 ka (Table 1).

Table 1: D_e values, dose rates and calculated pIRIR and IR-RF ages for the samples from Badahlin Cave (BDL2) and Gu Myaung Cave (GUMY).

Sample	Depth [cm]	Grain size [µm]	Number of grains [1]	Dose rate [Gy/ka]	Equivalent dose [Gy] [2]			Over-dispersion [%]	Age [ka] [3]		
					pIRIR	IR-RF (IRSAR)	IR-RF (RF_{70})		pIRIR	IR-RF (IRSAR)	IR-RF (RF_{70})
BDL2-OSL 3	80	90–125	1200/326	2.38 ± 0.13	71 ± 2	105 ± 24	129 ± 8	38 ± 2	29.9 ± 1.9	44.2 ± 10.4	54.3 ± 4.6
		180–212	300/47	2.60 ± 0.16	80 ± 3	-	-	35 ± 4	30.8 ± 2.3	-	-
BDL2-OSL 2	150	180–212	300/42	3.86 ± 0.20	203 ± 13	332 ± 13	343 ± 26	38 ± 5	52.5 ± 4.5	85.9 ± 5.9	88.8 ± 8.4
BDL2-OSL 1	240	180–212	300/80	3.85 ± 0.23	252 ± 12	346 ± 8	281 ± 13	39 ± 3	65.5 ± 5.1	89.9 ± 5.9	73.0 ± 5.6
GUMY-OSL 3	140	90–125	600/14	1.31 ± 0.10	33 ± 7	69 ± 4	93 ± 29	70 ± 15	25.4 ± 5.7	53.1 ± 4.9	59.9 ± 19.4
GUMY-OSL 2	202	90–125	600/37	1.31 ± 0.09	35 ± 4	71 ± 2	-	61 ± 8	26.8 ± 3.6	54.5 ± 4.1	-

[1] Number of grains measured / number of grains accepted for estimation of pIRIR D_e values.

[2] Equivalent dose (D_e) values were estimated using the central age model. The pIRIR D_e values were corrected for a small residual dose (see text). For IR-RF D_e estimation, 2–5 single aliquots were measured for each sample.

[3] Age uncertainties are expressed at 1σ and include a 2% systematic error to allow for possible bias associated with calibration of the laboratory beta sources.

4.3 Multi-grain IR-RF

Before determining D_e values using the IRSAR IR-RF procedure, we conducted several tests to determine the most appropriate measurement conditions. Previous studies have suggested that prolonged solar bleaching (step 2 in Table S1) is required to reset the IR-RF signal (e.g., 3 hr: Frouin et al., 2015, 2017). For our samples, however, we found that solar simulator bleaches of >1 hr did not cause a further increase in the IR-RF signal—that is, the IR-RF source traps were fully emptied by a solar simulator bleach of 1 hr (Fig. 4, left panel)—so we used a solar bleach time of 1 hr in this study. We also performed a pause duration test to determine the minimum delay time needed to eliminate phosphorescence before measuring the regenerated IR-RF signal (step 3 in Table S1). We found that, similar to Buylaert et al. (2012a), the phosphorescence signals of our samples are very weak compared to the IR-RF signal (Fig. S4), and we could not distinguish between the regenerated IR-RF signals measured after pauses of 15–60 min (Fig. 4, right panel). We concluded, therefore, that the effects of phosphorescence on the IR-RF signals of our samples were negligible after a pause time of 15 min, which we adopted to save machine time. We caution, however, that these settings are sample- and instrument-specific, and may not be appropriate for samples from other sites.

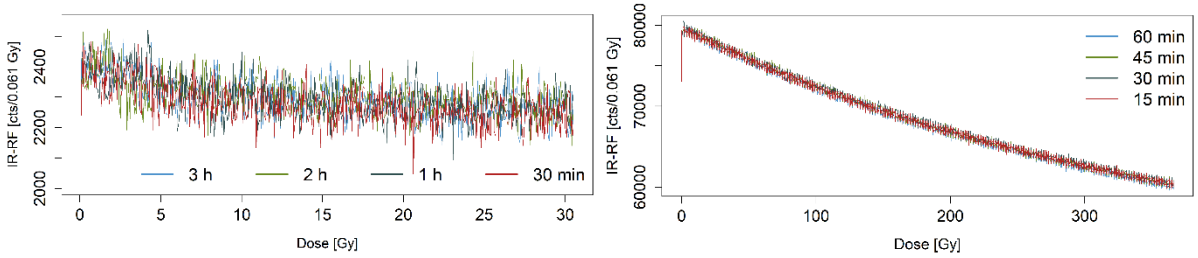

Figure 4. Test of solar bleaching time (left) and pause time (right) for IR-RF measurements of sample BDL2-OSL 3 using the IRSAR procedure (Table S1). In the first experiment (left panel), a used single aliquot was given a regenerative dose of ~305 Gy, bleached for duration t_b using the solar simulator in the Lexsyg reader, and paused for 1 hr before measuring the IR-RF signal. This cycle was repeated four times with t_b varied from 30 min to 3 hr. The left panel shows the early portion (0–30 Gy) of the IR-RF signal. In the second experiment (right panel), the same disc was first bleached for 1 hr using the solar simulator and paused for duration t_p before measuring the IR-RF signal. This cycle was repeated four times with t_p varied from 15 min to 60 min. Additional data are presented in Fig. S4.

To validate our revised procedures, we conducted dose recovery tests on natural aliquots of samples BDL2-OSL 3 (Fig. S5) and GUMY-OSL 3. We first bleached them for 4 hr in the solar simulator and then gave them beta

doses similar in size to the expected D_e values. The weighted-mean dose recovery ratios are 1.06 ± 0.03 and 1.31 ± 0.13, respectively. These results suggest that the given dose can be recovered with sufficient accuracy using the experimental conditions in our IRSAR procedure (Table S1) for samples from Badahlin Cave, but that the D_e values for the Gu Myaung Cave samples may be slightly overestimated.

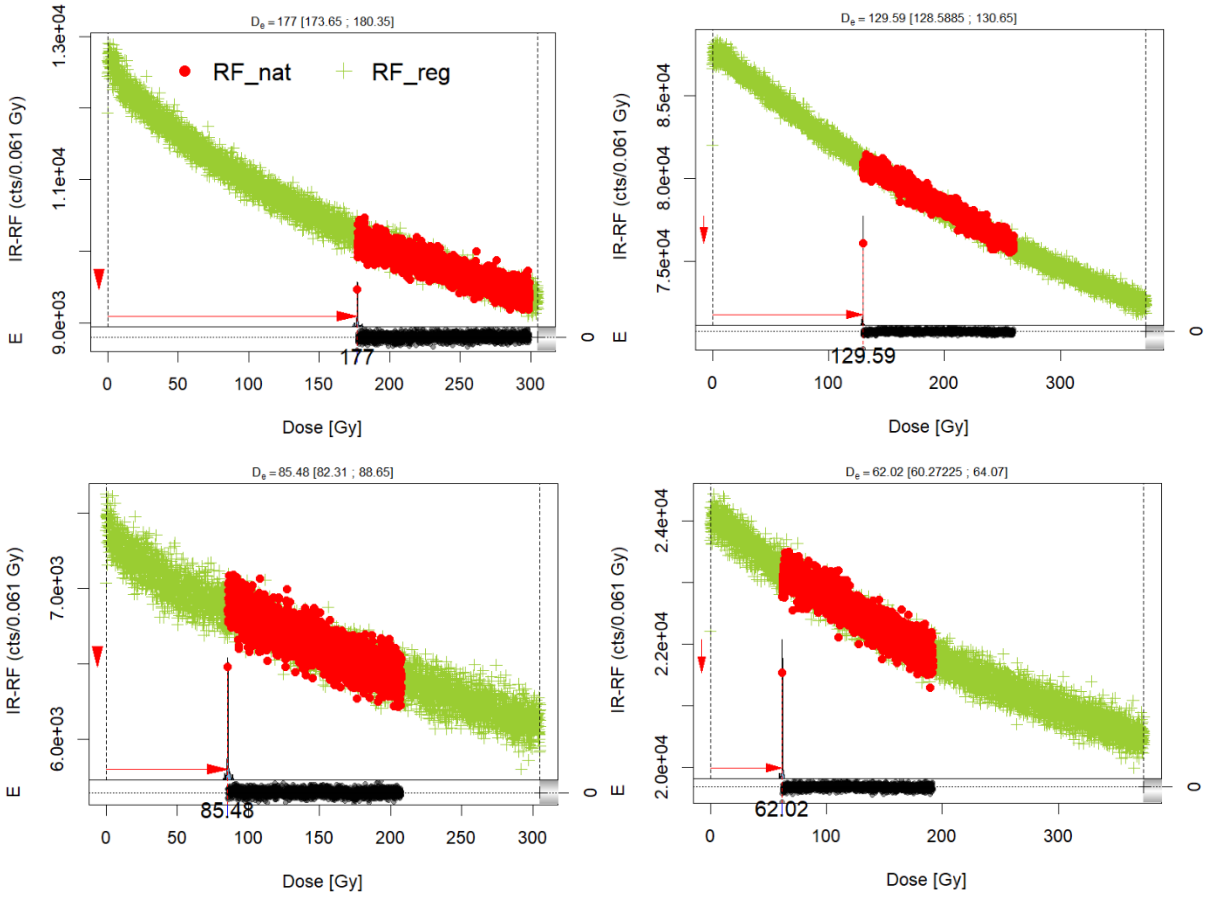

Figure 5: IRSAR and RF_{70} data for BDL2-OSL 3 from Badahlin Cave (top panels) and GUMY-OSL 3 from Gu Myaung Cave (bottom panels). The IRSAR D_e values are ~177 Gy (top left) and ~85 Gy (bottom left) for IRSAR, and ~130 Gy (top right) and ~62 Gy (bottom right) for RF_{70}.

We also tested the RF_{70} procedure (Frouin et al., 2017) on our samples. Preliminary tests showed that IR-RF measurements made at 70°C did not improve the shapes of the decay curves for our samples, in contrast to the findings of Huot et al. (2015) and Frouin et al. (2017). Nevertheless, the RF_{70} procedure yields slightly different results to those obtained using the IRSAR procedure: the RF_{70} signal intensity is higher and the calculated D_e values differ by 11–65 Gy, with the RF_{70} values being larger in some instances and smaller in

292 others (Table 1); two examples are shown in Fig. 5. The cause(s) of these differences are under investigation,
293 including tests of the suitability of the RF_{70} measurement conditions for our samples.

294 We estimated the IR-RF ages from the weighted-mean (CAM) D_e values for 2–5 aliquots of each sample,
295 without making any allowance for a residual dose (Table 1). The calculated ages for the Badahlin Cave samples
296 range from 44 ± 10 ka to 90 ± 6 ka (IRSAR) and from 54 ± 5 ka to 89 ± 8 ka (RF_{70}). The Gu Myaung Cave samples
297 yielded IRSAR ages of ~54 ka and, for GUMY-OSL 3, a RF_{70} age of 60 ± 19 ka. These ages are much older than
298 the pIRIR and ^{14}C chronologies, which is likely due to insufficient bleaching of the IR-RF signal. Subtraction of an
299 appropriate residual dose would likely reduce these age discrepancies considerably, and we are in the process
300 of assessing its likely size for these samples.

301

302 **5 Discussion**

303 In this preliminary study of K-feldspar grains from two archaeological sites in central Myanmar, we have shown
304 that the single-grain pIRIR procedure is suitable for dating, with acceptable results from dose recovery tests
305 and no evidence for fading of the pIRIR signal over laboratory timescales. There is potential, therefore, to
306 extend the applicability of pIRIR dating to other Palaeolithic sites in mainland Southeast Asia.

307 A comparison with independent (^{14}C) age control at Gu Myaung Cave has revealed, however, that both pIRIR
308 ages (~26 ka) significantly overestimate the ^{14}C ages (~10 and ~15 ka cal BP; Table S3) obtained for charcoal
309 fragments collected from stratigraphic layers between and below these two sediment samples (Fig. 2b).
310 Further evidence is required to validate which, if either, of these two chronologies is the more reliable. Our
311 residual dose test of K-feldspar grains from Badahlin and Gu Myaung Caves suggests that the pIRIR signal can
312 be (nearly) fully reset by solar bleaching in the laboratory, but this does imply that the sediments were, in fact,
313 exposed to sufficient sunlight when deposited at these sites. On the other hand, the pIRIR D_e distribution
314 patterns provide no support for heterogeneous bleaching (Fig. 3), so the causes of the age discrepancy at Gu
315 Myaung Cave remain elusive and are currently under investigation.

316 Duller (1994) proposed two types of poorly bleached sediments in nature: 1) sediments containing a mixture
317 of grains that have experienced differing degrees of bleaching—some grains being completely bleached at
318 deposition and others receiving little or no light exposure; and 2) sediments in which all grains have been

equally poorly bleached at deposition. If the discrepant pIRIR and ^{14}C ages at Gu Myaung Cave are due to insufficient bleaching of the pIRIR signal, then these samples may represent the second type of sediment, which could yield symmetric D_e distributions. We note, however, that this type of sediment is expected to be rare in natural environments (Wallinga, 2002).

In the case of Gu Myaung Cave, we consider it unlikely that all of the grains were poorly bleached, since the sediment samples were collected from an excavation located close to the cave entrance. To obtain further insights into the bleaching history of the sediments and whether the residual doses measured in the laboratory are representative of the sediments when deposited in the cave, we will conduct residual dose tests and examine the D_e distributions of recently deposited samples from the upper part of the stratigraphy. The reliability of the ^{14}C ages also warrants further investigation, and comparisons with chronologies constructed from complementary techniques (e.g., U-series dating of suitable flowstones) would be instructive.

The IR-RF ages obtained in this study consistently overestimate their pIRIR counterparts by 8–36 ka (Table 1), which we attribute to the different bleachabilities of these two signals. The use of multi-grain aliquots for IR-RF dating will exacerbate problems of D_e overestimation if partial bleaching is an issue. We note that the pIRIR and IRSAR IR-RF ages systematically increase with depth at Badahlin Cave, while the two pIRIR ages for Gu Myaung Cave are statistically indistinguishable, as are the two IR-RF ages at this site. This pattern suggests a common underlying cause for the age offset, which we are currently investigating. Other future lines of enquiry include further testing of the RF_{70} procedure of Frouin et al. (2017), including dose recovery tests and other variations to readout temperature, and processing of younger samples from both sites to obtain an improved estimate of the residual dose at deposition.

If our pIRIR ages for Badahlin Cave are accurate, then human occupation started at least ~30 ka ago (Fig.2a). The underlying, culturally sterile deposits dated to ~53 ka and ~66 ka might be interpreted as evidence that people had not arrived in this region by 53 ka, but we consider such inferences as premature given the many chambers of Badahlin Cave that have yet to be excavated. Sediments appear to have been accumulating in parts of the large cave complex for more than 50 millennia and further excavations may reveal earlier traces of human habitation. Based on our current pIRIR ages, occupation of Gu Myaung Cave appears to have commenced ~25 ka ago, whereas the ^{14}C chronology suggests human arrival during the early Holocene (Fig. 2b). In addition to resolving these discordant chronologies, future work may yet reveal a longer record of

human occupation of this site, which cannot be ruled out on the basis of the limited excavations conducted thus far.

6 Conclusions

We have applied single-grain pIRIR and multi-grain IR-RF dating procedures to K-feldspar extracts from archaeological deposits at Badahlin and Gu Myaung Caves in central Myanmar. Luminescence investigations of the pIRIR and IR-RF signals, and the corresponding D_e distributions, indicates that the pIRIR procedure, at least, may be suitable for sediment dating. The IR-RF ages overestimate the pIRIR D_e values and ages by a considerable margin, which may be related to the poorer bleachability and higher residual doses associated with the IR-IF signal. Even the pIRIR ages are substantially older than the ^{14}C ages at Gu Myaung Cave, despite the lack of support for heterogeneous bleaching in the single-grain D_e distributions. Future investigations could involve pIRIR and IR-RF measurements of recently deposited sediments to determine the residual doses at deposition in the natural environment, and IR-RF measurements of individual K-feldspar grains (e.g., Trautmann et al., 2000) to avoid the shortcomings of using multi-grain aliquots to date partially bleached sediments. Our preliminary pIRIR chronologies indicate that human occupation of Badahlin and Gu Myaung Caves started at least ~30 ka and ~25 ka ago, respectively, thereby adding to the sparse chronological record supporting Palaeolithic settlement of the region during the Late Pleistocene (Aung et al., 2015).

Acknowledgements

This study was funded by the Australian Research Council through an Australian Laureate Fellowship to R.G.R. (FL130100116) and Future Fellowships to B.L. (FT140100384) and B.M. (FT140100101), and by the University of Wollongong through a Postgraduate Award and an International Postgraduate Research Scholarship to M.S. The radiocarbon analyses were funded by the European Research Council under the European Union's Seventh Framework Programme (FP7/2007-2013)/ERC grant agreement no. 324139 ('PalaeoChron' project to T. Higham). We also thank Zaw Phyo, Tin Thut Aung, May Su Ko, Hu Yue, Myo Thi Ha and Yin Min for assisting with the excavations, and the teams in the luminescence laboratories at the University of Wollongong (Australia) and the University of Bayreuth (Germany) for assisting with sample preparation and measurement.

374 **References**

375 Auclair, M., Lamothe, M., Huot, S., 2003. Measurement of anomalous fading for feldspar IRSL using SAR.
376 Radiat. Meas. 37, 487–492. doi:10.1016/S1350-4487(03)00018-0

377 Aung Thaw, U., 1971. The "Neolithic" Culture of the Padah-lin Caves. Asian Perspect. 14, 123–133.

378 Aung-Thwin, M., 2001. Origins and development of the field of prehistory in Burma. Asian Perspect. 40, 6–34.
379 doi:10.1353/asi.2001.0002

380 Aung, T.H., Marwick, B., Conrad, C., 2015. Palaeolithic zooarchaeology in Myanmar: a review and future
381 prospects. J. Indo-Pacific Archaeol. 39, 50–56. doi:10.7152/jipa.v39i0.14896

382 Blegen, N., Tryon, C.A., Faith, J.T., Peppe, D.J., Beverly, E.J., Li, B., Jacobs, Z., 2015. Distal tephras of the eastern
383 Lake Victoria basin, equatorial East Africa: correlations, chronology and a context for early modern
384 humans. Quat. Sci. Rev. 122, 89–111. doi:10.1016/j.quascirev.2015.04.024

385 Bøtter-Jensen, L., Mejdahl, V., 1988. Assessment of beta dose rate using a GM multicounter system. Nucl.
386 Tracks Radiat. Meas. 14, 187–191. doi:10.1016/1359-0189(88)90062-3

387 Bøtter-Jensen, L., Andersen, C.E., Duller, G.A.T., Murray, A.S., 2003. Developments in radiation, stimulation and
388 observation facilities in luminescence measurements. Radiat. Meas. 37, 535–541. doi: 10.1016/S1350-
389 4487(03)00020-9

390 Buylaert, J.P., Jain, M., Murray, A.S., Thomsen, K.J., Lapp, T., 2012a. IR-RF dating of sand-sized K-feldspar
391 extracts: a test of accuracy. Radiat. Meas. 47, 759–765. doi:10.1016/j.radmeas.2012.06.021

392 Buylaert, J.P., Jain, M., Murray, A.S., Thomsen, K.J., Thiel, C., Sohbati, R., 2012b. A robust feldspar
393 luminescence dating method for Middle and Late Pleistocene sediments. Boreas 41, 435–451.
394 doi:10.1111/j.1502-3885.2012.00248.x

395 Colarossi, D., Duller, G.A.T., Roberts, H.M., Tooth, S., Lyons, R., 2015. Comparison of paired quartz OSL and
396 feldspar post-IR IRSL dose distributions in poorly bleached fluvial sediments from South Africa. Quat.
397 Geochronol. 30, 233–238. doi:10.1016/j.quageo.2015.02.015

398 Demeter, F., Shackelford, L., Westaway, K., Duringer, P., Bacon, A.M., Ponche, J.L., Wu, X., Sayavongkhamdy,
399 T., Zhao, J.X., Barnes, L., Boyon, M., Sichanthongtip, P., Sénégas, F., Karpoff, A.M., Patole-Edoumba, E.,

Coppens, Y., Braga, J., 2015. Early modern humans and morphological variation in Southeast Asia: fossil evidence from Tam Pa Ling, Laos. PLoS One 10, e0121193. doi:10.1371/journal.pone.0121193

Duller, G.A.T., 1994. Luminescence dating of poorly bleached sediments from Scotland. Quat. Geochronol. 13, 521–524. doi:10.1016/0277-3791(94)90070-1

Erfurt, G., Krbetschek, M.R., 2003. IRSAR – A single-aliquot regenerative-dose dating protocol applied to the infrared radiofluorescence (IR-RF) of coarse-grain K feldspar. Anc. TL 21, 35–42.

Forestier, H., Sophady, H., Puaud, S., Celiberti, V., Frere, S., Zeitoun, V., Mourer-Chauvire, C., Mourer, R., Than, H., Billault, L., 2015. The Hoabinhian from Laang Spean Cave in its stratigraphic, chronological, typo-technological and environmental context (Cambodia, Battambang province). J. Archaeol. Sci. Reports 3, 194–206. doi:10.1016/j.jasrep.2015.06.008

Frouin, M., Huot, S., Mercier, N., Lahaye, C., Lamothe, M., 2015. The issue of laboratory bleaching in the infrared-radiofluorescence dating method. Radiat. Meas. 81, 212–217. doi:10.1016/j.radmeas.2014.12.012

Frouin, M., Huot, S., Kreutzer, S., Lahaye, C., Lamothe, M., Philippe, A., Mercier, N., 2017. An improved radiofluorescence single-aliquot regenerative dose protocol for K-feldspars. Quat. Geochronol. 38, 13–24. doi:10.1016/j.quageo.2016.11.004

Fu, X., 2014. The D_e (T, t) plot: a straightforward self-diagnose tool for post-IR IRSL dating procedures. Geochronometria 41, 315–326. doi:10.2478/s13386-013-0167-9

Galbraith, R.F., Roberts, R.G., 2012. Statistical aspects of equivalent dose and error calculation and display in OSL dating: an overview and some recommendations. Quat. Geochronol. 11, 1–27. doi:10.1016/j.quageo.2012.04.020

Galbraith, R.F., Roberts, R.G., Laslett, G.M., Yoshida, H., Olley, J.M., 1999. Optical dating of single and multiple grains of quartz from Jinmium rock shelter, northern Australia: Part I, experimental design and statistical models. Archaeometry 41, 339–364. doi:10.1111/j.1475-4754.1999.tb00987.x

Galbraith, R.F., Roberts, R.G., Yoshida, H., 2005. Error variation in OSL palaeodose estimates from single aliquots of quartz: a factorial experiment. Radiat. Meas. 39, 289–307. doi:

426 10.1016/j.radmeas.2004.03.023

427 Guérin, G., Mercier, N., Nathan, R., Adamiec, G., Lefrais, Y., 2012. On the use of the infinite matrix assumption
428 and associated concepts: a critical review. Radiat. Meas. 47, 778–785.
429 doi:10.1016/j.radmeas.2012.04.004

430 Huntley, D.J., Hancock, R.G. V., 2001. The Rb contents of the K-feldspar grains being measured in optical
431 dating. Anc. TL 19, 43–46.

432 Huot, S., Frouin, M., Lamothe, M., 2015. Evidence of shallow TL peak contributions in infrared
433 radiofluorescence. Radiat. Meas. 81, 237–241. doi:10.1016/j.radmeas.2015.05.009

434 Jacobs, Z., Roberts, R.G., 2007. Advances in optically stimulated luminescence dating of individual grains of
435 quartz from archeological deposits. Evol. Anthropol. 16, 210–223. doi:10.1002/evan.20150

436 Jacobs, Z., Roberts, R.G., 2015. An improved single grain OSL chronology for the sedimentary deposits from
437 Diepkloof Rockshelter, Western Cape, South Africa. J. Archaeol. Sci. 63, 175–192.
438 doi:10.1016/j.jas.2015.01.023

439 Krbetschek, M.R., Trautmann, T., Dietrich, A., Stolz, W., 2000. Radioluminescence dating of sediments:
440 methodological aspects. Radiat. Meas. 32, 493–498. doi:10.1016/S1350-4487(00)00122-0

441 Kreutzer, S., Dietze, M., Burow, C., Fuchs, M.C., Schmidt, C., Fischer, M., Friedrich, J., Mercier, N., Smedley,
442 R.K., Christophe, C., Zink, A., Durcan, J., King, G., Philippe, A., Guerin, G., Fuchs, M., 2017. Luminescence:
443 Comprehensive Luminescence Dating Data Analysis. R package version 0.7.5. https://CRAN.R-
444 project.org/package=Luminescence

445 Li, B., Li, S.-H., 2011. Luminescence dating of K-feldspar from sediments: a protocol without anomalous fading
446 correction. Quat. Geochronol. 6, 468–479. doi:10.1016/j.quageo.2011.05.001

447 Li, B., Li, S.-H., 2012. A reply to the comments by Thomsen et al . on “Luminescence dating of K-feldspar from
448 sediments: a protocol without anomalous fading correction” 8, 49–51.
449 doi:10.1016/j.quageo.2011.10.001

450 Li, B., Jacobs, Z., Roberts, R.G., Li, S.-H., 2014. Review and assessment of the potential of post-IR IRSL dating
451 methods to circumvent the problem of anomalous fading in feldspar luminescence. Geochronometria

452 41, 178–201. doi: 10.2478/s13386-013-0160-3

453 Moncel, M.-H., Arzarello, M., Boëda, É., Bonilauri, S., Chevrier, B., Gaillard, C., Forestier, H., Yinghua, L., Sémah,
454 F., Zeitoun, V., 2016. Assemblages with bifacial tools in Eurasia (second part). What is going on in the
455 East? Data from India, Eastern Asia and Southeast Asia. Comptes Rendus Palevol.
456 doi:http://dx.doi.org/10.1016/j.crpv.2015.09.010

457 Nathan, R.P., Mauz, B., 2008. On the dose-rate estimate of carbonate-rich sediments for trapped charge
458 dating. Radiat. Meas. 43, 14–25. doi:10.1016/j.radmeas.2007.12.012

459 Novothny, A., Frechen, M., Horvath, E., Krbetschek, M.R., Tsukamoto, S., 2010. Infrared stimulated
460 luminescence and radiofluorescence dating of aeolian sediments from Hungary. Quat. Geochronol. 5,
461 114–119. doi:10.1016/j.quageo.2009.05.002

462 Prescott, J.R., Hutton, J.T., 1994. Cosmic ray contributions to dose rates for luminescence and ESR dating: large
463 depths and long-term time variations. Radiat. Meas. 23, 497–500. doi:10.1016/1350-4487(94)90086-8

464 Readhead, M.L., 1987. Thermoluminescence dose rate data and dating equations for the case of disequilibrium
465 in the decay series. Nucl. Tracks Radiat. Meas. 13, 197–207. doi: 10.1016/1359-0189(87)90037-9

466 Reimann, T., Thomsen, K.J., Jain, M., Murray, A.S., Frechen, M., 2012. Single-grain dating of young sediments
467 using the pIRIR signal from feldspar. Quat. Geochronol. 11, 28–41. doi:10.1016/j.quageo.2012.04.016

468 Rhodes, E.J., 2015. Dating sediments using potassium feldspar single-grain IRSL: initial methodological
469 considerations. Quat. Int. 362, 14–22. doi:10.1016/j.quaint.2014.12.012

470 Richter, D., Pintaske, R., Dornich, K., Krbetscheck, M., 2012. A novel beta source design for uniform irradiation
471 in dosimetric applications. Anc. TL 30, 57–64.

472 Richter, D., Richter, A., Dornich, K., 2013. Lexsyg — A new system for luminescence research. Geochronometria
473 40, 220–228. doi:10.2478/s13386-013-0110-0

474 Roberts, R.G., Morwood, M.J., Westaway, K.E., 2005. Illuminating Southeast Asian prehistory: new
475 archaeological and paleoanthropological frontiers for luminescence dating. Asian Perspect. 44, 293–319.
476 doi:10.1353/asi.2005.0028

477 Roberts, R.G., Jacobs, Z., Li, B., Jankowski, N.R., Cunningham, A.C., Rosenfeld, A.B., 2015. Optical dating in

archaeology: thirty years in retrospect and grand challenges for the future. J. Archaeol. Sci. 56, 41–60. doi:10.1016/j.jas.2015.02.028

Smedley, R.K., Duller, G.A.T., Pearce, N.J.G., Roberts, H.M., 2012. Determining the K-content of single-grains of feldspar for luminescence dating. Radiat. Meas. 47, 790–796. doi:10.1016/j.radmeas.2012.01.014

Trauerstein, M., Lowick, S.E., Preusser, F., Schlunegger, F., 2014. Small aliquot and single grain IRSL and post-IR IRSL dating of fluvial and alluvial sediments from the Pativilca valley, Peru. Quat. Geochronol. 22, 163–174. doi:10.1016/j.quageo.2013.12.004

Trautmann, T., Krbetschek, M.R., Dietrich, A., Stolz, W., 1998. Investigations of feldspar radioluminescence: potential for a new dating technique. Radiat. Meas. 29, 421–425. doi:10.1016/S1350-4487(98)00012-2

Trautmann, T., Dietrich, A., Stolz, W., Krbetschek, M.R., 1999a. Radioluminescence dating: a new tool for Quaternary geology and archaeology. Naturwissenschaften 86, 441–444. doi:10.1007/s001140050649

Trautmann, T., Krbetschek, M.R., Dietrich, A., Stolz, W., 1999b. Feldspar radioluminescence: a new dating method and its physical background. J. Lumin. 85, 45–58. doi:10.1016/S0022-2313(99)00152-0

Trautmann, T., Krbetschek, M.R., Stolz, W., 2000. A systematic study of the radioluminescence properties of single feldspar grains. Radiat. Meas. 32, 685–690. doi: 10.1016/S1350-4487(00)00077-9

Wallinga, J., 2002. Optically stimulated luminescence dating of fluvial deposts: a review. Boreas 31, 303–322. doi:10.1111/j.1502-3885.2002.tb01076.x

Yi, S., Buylaert, J.P., Murray, A.S., Lu, H., Thiel, C., Zeng, L., 2016. A detailed post-IR IRSL dating study of the Niuyangzigou loess site in northeastern China. Boreas 45, 644–657. doi:10.1111/bor.12185

Supplementary data

Table S1. *D_e measurement procedures used in this study.*

Step	pIRIR	IR-RF (IRSAR)	IR-RF (RF_{70})
1	Natural or regenerative dose	Natural IR-RF (room temperature)	Preheat (70°C for 120 s)
2	Preheat (320°C for 60 s)	Solar simulator bleach (3600 s) [1]	Natural IR-RF (70°C)
3	IRSL (200°C for 100 s)	Pause (1000 s)	Solar simulator bleach (3600 s) [1]
4	SG pIRIR (275°C for 1.5 s)	Regenerated IR-RF (room temperature)	Pause (1000 s)
5	Test dose		Preheat (70°C for 120 s)
6	Preheat (320°C for 60 s)		Regenerated IR-RF (70°C)
7	IRSL (200°C for 100 s)		
8	SG pIRIR (275°C for 1.5 s)		
9	IR bleach (340°C for 100 s)		
10	Return to step 1		

[1] Solar simulator bleach settings after Frouin et al. (2015): 365 nm (10 mW/cm^2), 462 nm (63 mW/cm^2), 525 nm (54 mW/cm^2), 590 nm (37 mW/cm^2), 623 nm (115 mW/cm^2) and 850 nm (96 mW/cm^2).

Table S2. *Dose rate information for the samples from Badahlin Cave (BDL2) and Gu Myaung Cave (GUMY).*

Sample	Grain size [μm]	Moisture [%]	Internal [Gy/ka]	Beta [Gy/ka]	Gamma [Gy/ka]	Cosmic [Gy/ka][1]	Total dose rate [Gy/ka]
BDL2-OSL 3	90–125	27	0.38 ± 0.08	1.21 ± 0.08	0.79 ± 0.05	–	2.38 ± 0.13
	180–212		0.67 ± 0.12	1.14 ± 0.08		–	2.60 ± 0.16
BDL2-OSL 1	180–212	27	0.67 ± 0.12	2.11 ± 0.15	1.09 ± 0.08	–	3.86 ± 0.20
BDL2-OSL 2		37		1.90 ± 0.16	1.28 ± 0.10	–	3.85 ± 0.23
GUMY-OSL 3	90–125	18	0.38 ± 0.08	0.63 ± 0.04	0.27 ± 0.02	0.02 ± 0.01	1.31 ± 0.10
GUMY-OSL 2		14		0.62 ± 0.03	0.29 ± 0.01		1.31 ± 0.09

[1] Cosmic-ray dose rates in Badahlin Cave are negligible due to strong attenuation by ~30 m of rock shielding.

Radiocarbon dating

Three unidentified charcoal samples were submitted for ^{14}C dating to the Oxford Radiocarbon Accelerator Unit. The samples underwent microscopic investigation and visual inclusions were removed using clean tweezers.

Between 20 and 30 mg of charcoal underwent the new AOx-SC protocol (Douka et al., in preparation), identified with the YR code at ORAU. The AOx-SC protocol is a modification of the ABOx-SC procedure *(Bird et al., 1999; Brock et al., 2010)*, which is harsher on samples, resulting in a much higher failure rate and a need for larger sample sizes. Samples were given an initial wash with 6 M HCl acid for 1 hr at room temperature, followed by oxidisation in $H_2SO_4/K_2Cr_2O_7$ (2 M/0.1 M) at 60°C in a sealed tube for 20 hr. The charcoal was washed three times with ultrapure water between each treatment. Unlike the ABOx-SC procedure, the AOx-SC protocol does not include a NaOH step. After freeze-drying, the charcoal was loaded into a quartz tube topped by quartz wool (previously baked at 850°C for 8 hr) and combusted to 630°C for 2 hr. A second combustion at 1000°C followed in a CHN elemental analyser (Carlo-Erba NA, 2000) coupled to a gas source isotope ratio mass spectrometer (Sercon 20/20), enabling online measurement of carbon elemental ratios and stable isotopes. CO_2 gas was collected and reduced with H_2 to produce graphite (Dee and Bronk Ramsey, 2000) prior to measurement by accelerator mass spectrometry. The conventional ages are listed in Table S3 (in years before present, BP, where the 'present' is defined as AD 1950), together with calibrated age ranges at the 68.2% and 95.4% confidence intervals. Calibrations were performed using the IntCal13 dataset (Reimer et al., 2013) and the OxCal program (Bronk Ramsey, 2009; Bronk Ramsey and Lee, 2013).

Table S3. *Radiocarbon ages for charcoal samples from Gu Myaung Cave.*

Laboratory code	Field sample ID	Age [years BP]	Calibrated age ranges [years cal BP]	
			68.2% CI	95.4% CI
OxA-34804	GM-C14-14	12,665 ± 55	14,974–15,197	14,790–15,261
OxA-34805	GM-C14-16	9,240 ± 40	10,374–10,496	10,261–10,520
OxA-34806	GM-C14-26	2,829 ± 28	2,917–2,962	2,854–3,005

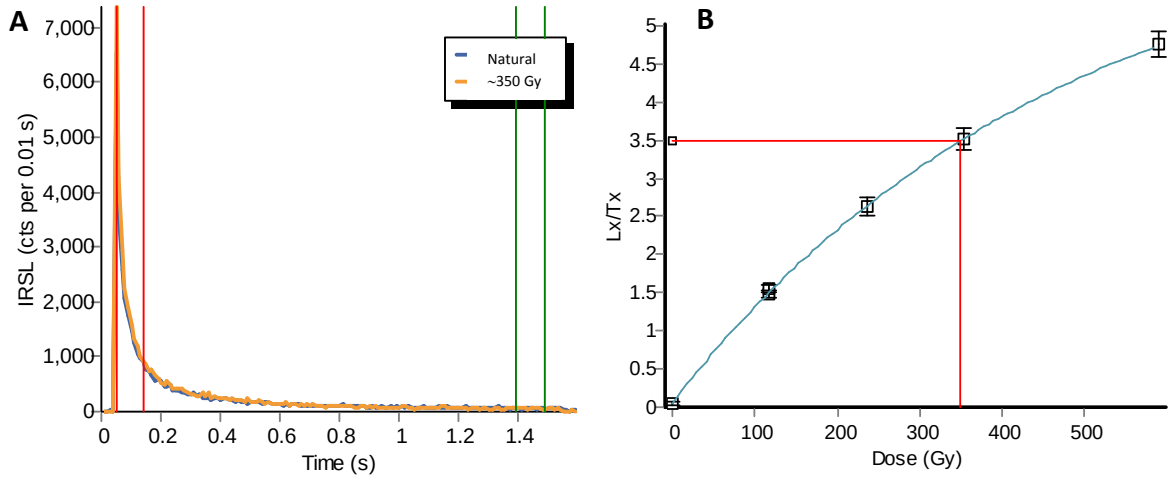

Figure S1. *Representative pIRIR decay curve (A) and dose response curve (B) for a single grain of K-feldspar from sample BDL2-OSL 2, measured using the pIRIR procedure in Table S1.*

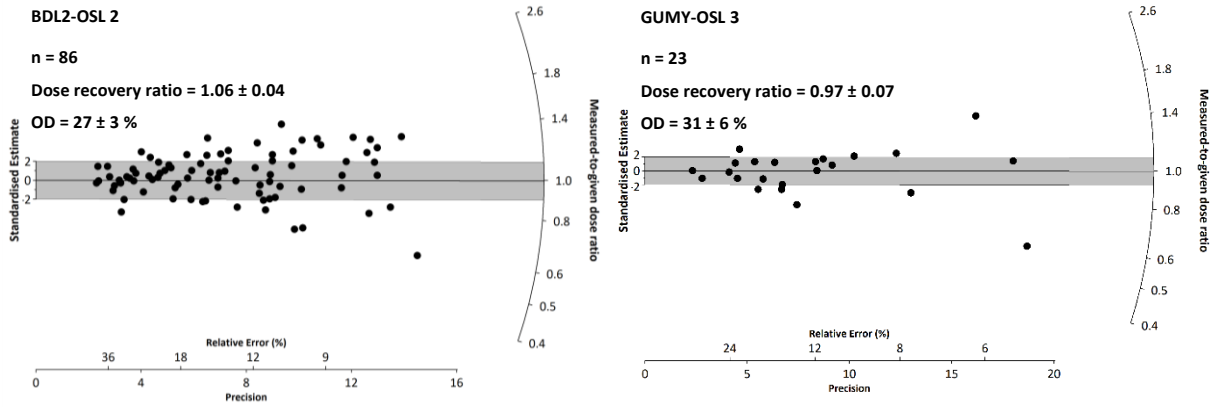

Figure S2. *Results of single-grain pIRIR dose recovery tests on samples BDL2-OSL 2 (left) and GUMY-OSL 3 (right). Natural K-feldspar grains were bleached for 4 hr using a Dr Hönle UVACUBE 400 solar simulator and then given a beta dose close the expected natural D_e of the sample (236 Gy for BDL2-OSL 2 and 30 Gy for GUMY-OSL 3). These surrogate natural doses were measured using the single-grain pIRIR procedure in Table S1. The grey bands in the radial plots are centred on a dose recovery ratio of unity (i.e., ratio of measured dose to given dose = 1).*

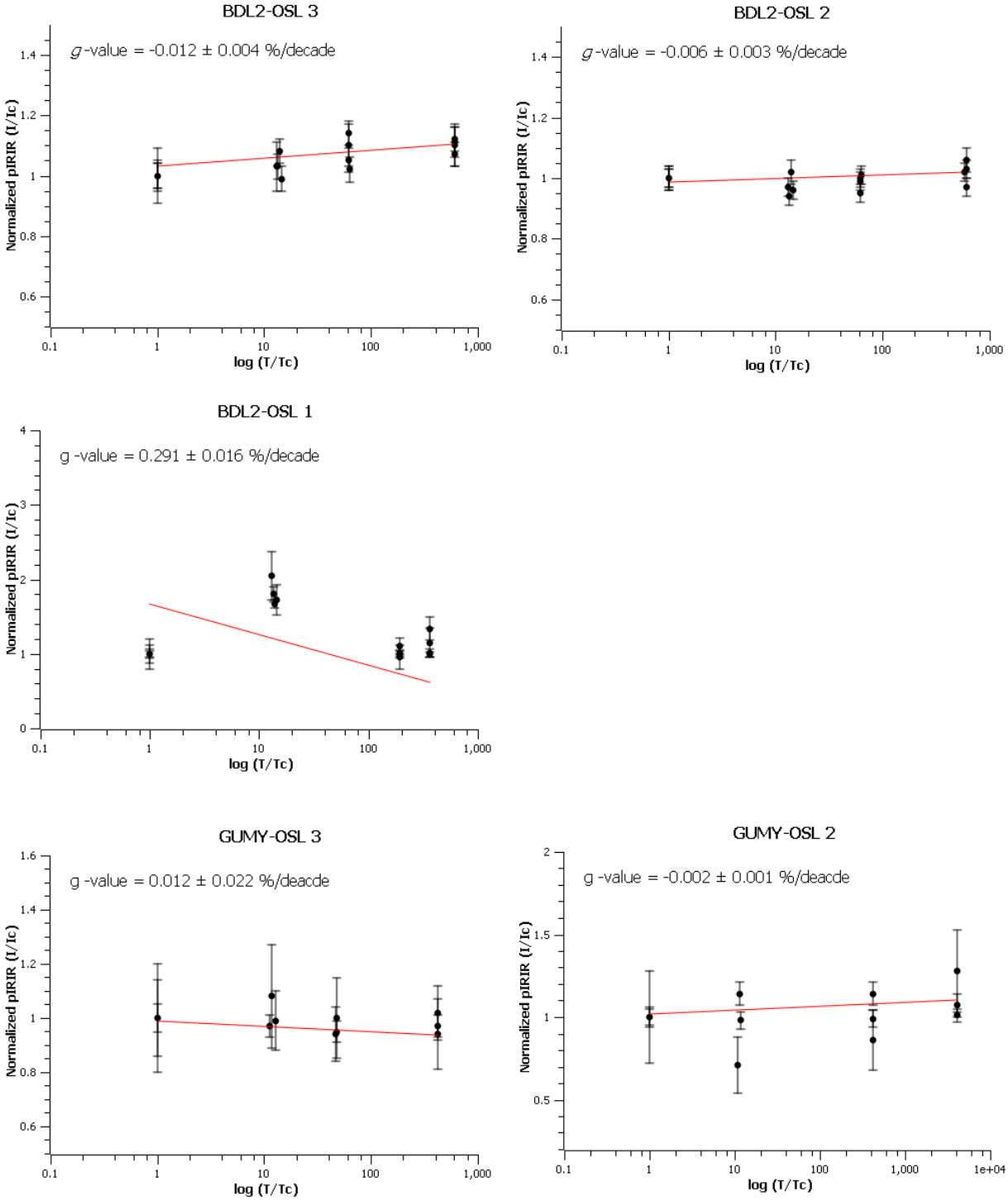

Figure S3. *Results of anomalous fading tests for pIRIR signals of all samples. Fading tests were performed on multi-grain aliquots following Auclair et al. (2003) using a regenerative dose of ~235 Gy. The pause durations varied from a few minutes (directly after irradiation) to 2 weeks. The g-values are normalised to t_c = time of first measurement (i.e. immediate measurement after irradiation). All samples show a fading rate varying between ~0 and 0.3 % per decade.*

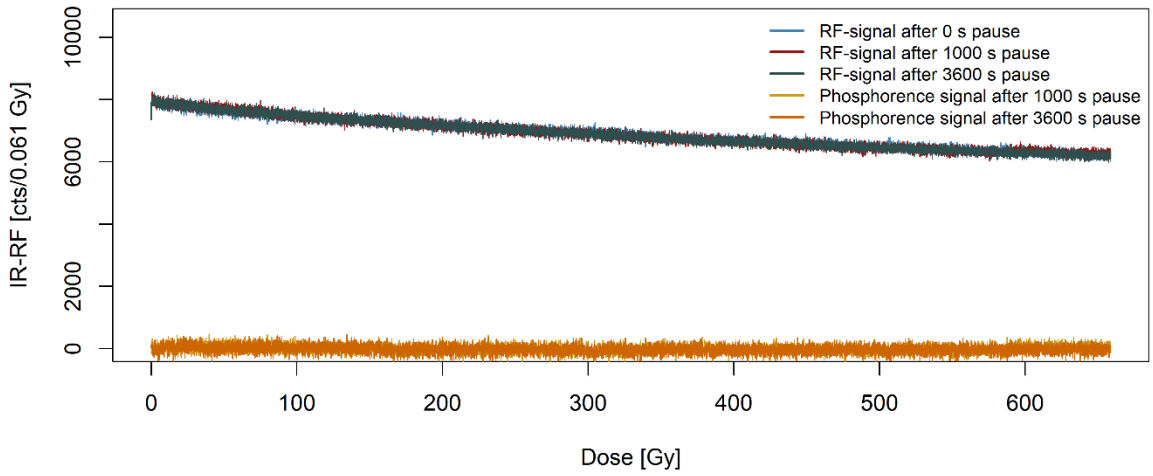

Figure S4. *The effect of phosphorescence on the IR-RF signal after different pause times. The regenerated IR-RF signal was measured multiple times using the IRSAR procedure in Table S1, with different pause times between the solar bleach and the IR-RF measurement: 0 s (blue), 1000 s (red), 3600 s (grey). The yellow and orange curves show the phosphorescence signal after pause times of 1000 s and 3600 s, obtained by subtracting the post-pause IR-RF signal from the IR-RF signal. The phosphorescence signal is negligible compared to the IR-RF signal.*

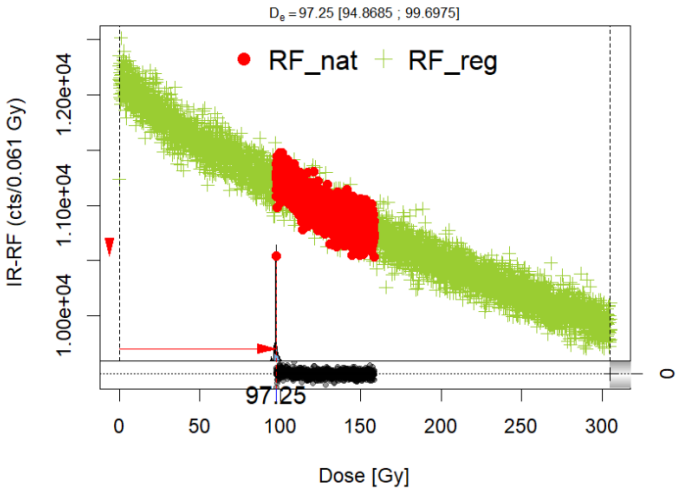

Figure S5. *Result of IR-RF (IRSAR) dose recovery test using an aliquot of sample BDL2-OSL 3. The given (surrogate natural) dose was ~92 Gy and the recovered dose was ~97 Gy, which yields a measured-to-given dose ratio of ~1.06. The natural signal is shown in red and the regenerated signal in green. The measured dose was estimated by horizontally and vertically shifting (red arrows) the surrogate natural signal to match the regenerated signal and minimise the residuals (black curve).*

References

Bird, M.I., Ayliffe, L.K., Fifield, L.K., Turney, C.S.M., Cresswell, R.G., Barrows, T.T., David, B., 1999. Radiocarbon dating of “old” charcoal using a wet oxidation, stepped-combustion procedure. Radiocarbon 41, 127–140. doi: 10.1017/S0033822200019482

Brock, F., Higham, T., Ditchfield, P., Ramsey, C.B., 2010. Current pretreatment methods for AMS radiocarbon dating at the Oxford Radiocarbon Accelerator Unit (ORAU). Radiocarbon 52, 103–112. doi:10.1017/S0033822200045069

Bronk Ramsey, C., 2009. Bayesian analysis of radiocarbon dates. Radiocarbon 51, 337–360. doi:10.2458/azu_js_rc.v51i1.3494

Bronk Ramsey, C., Lee, S., 2013. Recent and planned developments of the program OxCal. Radiocarbon 55, 720–730. do: 10.2458/azu_js_rc.55.16215

Dee, M., Bronk Ramsey, C., 2000. Refinement of graphite target production at ORAU. Nucl. Instr. Meth. Phys. Res. B 172, 449–453. doi:10.1016/S0168-583X(00)00337-2

Frouin, M., Huot, S., Mercier, N., Lahaye, C., Lamothe, M., 2015. The issue of laboratory bleaching in the infrared-radiofluorescence dating method. Radiat. Meas. 81, 212–217. doi:10.1016/j.radmeas.2014.12.012

Reimer, P.J., Bard, E., Bayliss, A., Beck, J.W., Blackwell, P.G., Ramsey, C.B., Buck, C.E., Cheng, H., Edwards, R.L., Friedrich, M., Grootes, P.M., Guilderson, T.P., Haflidason, H., Hajdas, I., Hatté, C., Heaton, T.J., Hoffmann, D.L., Hogg, A.G., Hughen, K.A., Kaiser, K.F., Kromer, B., Manning, S.W., Niu, M., Reimer, R.W., Richards, D.A., Scott, E.M., Southon, J.R., Staff, R.A., Turney, C.S.M., van der Plicht, J., 2013. IntCal13 and Marine13 radiocarbon age calibration curves 0–50,000 years cal BP. Radiocarbon 55, 1869–1887. doi:10.2458/azu_js_rc.55.16947